NeuroImage: Clinical 9 (2015) 479–483

Contents lists available at ScienceDirect

NeuroImage: Clinical

journal homepage: www.elsevier.com/locate/ynicl

Reduced binding of Pittsburgh Compound-B in areas of white matter hyperintensities

A.E. Goodheart[a], E. Tamburo[a], D. Minhas[b], H.J. Aizenstein[a], E. McDade[c], B.E. Snitz[c], J.C. Price[b], C.A. Mathis[b], O.L. Lopez[c], W.E. Klunk[a,c], A.D. Cohen[a,*]

[a]Department of Psychiatry, University of Pittsburgh School of Medicine, Pittsburgh, USA
[b]Department of Radiology, University of Pittsburgh School of Medicine, Pittsburgh, USA
[c]Department of Neurology, University of Pittsburgh School of Medicine, Pittsburgh, PA 15213, USA

ARTICLE INFO

Article history:
Received 10 February 2015
Received in revised form 28 July 2015
Accepted 10 September 2015
Available online 29 September 2015

Keywords:
white matter hyperintensities
PiB
Amyloid imaging
PET

ABSTRACT

The amyloid imaging agent, Pittsburgh Compound-B, binds with high affinity to β-amyloid (Aβ) in the brain, and it is well established that PiB also shows non-specific retention in white matter (WM). However, little is known about retention of PiB in areas of white matter hyperintensities (WMH), abnormalities commonly seen in older adults. Further, it is hypothesized that WMH are related to both cognitive dysfunction and Aβ deposition. The goal of the present study was to explore PiB retention in both normal-appearing WM (NAWM) and WMH in a group of elderly, cognitively normal individuals. In a group of cognitively normal elderly ($n = 64$; 86.5 ± 2.6 years) two analyses were applied: (1) ROIs were placed over periventricular areas in which WMH caps are commonly seen on all subjects, regardless of WMH burden or size. (2) Subject-specific maps of NAWM and WMH were co-registered with the PiB-PET images and mean SUVR values were calculated in these NAWM and WMH maps. PiB retention was significantly reduced in the ROIs of subjects with high WMH compared to subjects with low WMH. Additionally, in subjects with high WMH, there was significantly lower PiB retention in subject-specific maps of WMH compared to NAWM, which was not observed in subjects with low WMH, likely because of the small size of WMH maps in this group. These data suggest that WM in areas of WMH binds PiB less effectively than does normal WM. Further exploration of this phenomenon may lead to insights about the molecular basis of the non-specific retention of amyloid tracers in white matter.

1. Introduction

Pittsburgh Compound-B binds with high affinity to fibrillar amyloid-beta (Aβ) in the brain (Mathis et al., 2013). Thus, PiB provides a method of detecting and quantifying β-amyloid deposition in living subjects (Klunk et al., 2004). PiB studies have shown a 2-fold increase in tracer retention in Alzheimer disease (AD) cases compared to cognitively normal controls (for review see Cohen et al., 2012). Further, it also well established that PiB shows significant white matter retention, but this binding does not appear to be related to Aβ deposits (Klunk et al., 2004), and, interestingly, the absence of PiB has been shown to mark demyelinating lesions in models of multiple sclerosis and in humans with multiple sclerosis (Stankoff et al., 2011).

Little is known, however, about retention of PiB in areas of white matter hyperintensities (WMH). WMH are areas of increased signal intensity seen on T2-weighted magnetic resonance (MR) images (Gorelick et al., 2011). While the precise aetiology of WMH is debated (Scarpelli et al., 1994; Scheltens et al., 1995), these abnormalities are commonly thought to be a manifestation of subclinical vascular disease (Gorelick et al., 2011). Additionally, WMH are one of the most common pathological changes associated with aging (de Leeuw et al., 2001), and the presence of WMHs have been reported as risk factor for mild cognitive impairment (MCI) and AD (Yoshita et al., 2006). Neuropathologically, WMH have correlated primarily with demyelination but also with arteriosclerosis, axon loss, gliosis, dilated perivascular spaces, spongiosis, and lacunar infarcts (Chimowitz et al., 1992; Munoz et al., 1993; Scarpelli et al., 1994; Young et al., 2008). In a recent pathological study of cognitively normal controls, it was observed that vacuolation, decreased myelin density and decreased small vessel density contribute to the presence of WMH, while factors such as axonal density and glial cell burden did not (Murray et al., 2012). Further, posterior WMH have been found to be associated pathologically confirmed cerebral amyloid angiopathy (Thanprasertsuk et al., 2014).

Given the importance of both amyloid deposition and white matter lesions in the pathogenesis of AD and normal aging, it is critical to understand the binding properties of PiB to both normal and abnormal white matter. The goal of the present report is to explore PiB retention

* Corresponding author at: 1406 Western Psychiatric Institute and Clinic, Pittsburgh 15213, USA. Tel.: +1 412 246 6251; fax: +1 412 246 6466.

http://dx.doi.org/10.1016/j.nicl.2015.09.009

in both normal-appearing WM (NAWM) and WMH in a group of elderly, cognitively normal individuals.

2. Materials and methods

2.1. Human subjects

Participants were recruited from the Ginkgo Evaluation of Memory Study (GEMS, September 2000 through April 2008), a multisite, placebo-controlled, double-blind, randomized clinical trial of the daily use of Ginkgo biloba in 3069 community-dwelling participants aged 72–96 years at baseline (DeKosky et al., 2006). From July 2010 through November 2012, a total of 81 of these participants who remained nondemented were recruited for a neuroimaging assessment. For these analyses, we included the 64 cognitively normal elderly participants from this substudy, that were studied with PiB-PET, had visual WMH scores (Longstreth et al., 1996) and had FLAIR MRIs available for analysis. The average age of this subset of the complete cohort ($n = 64$) was 86.5 ± 2.6 years. All subjects were defined as cognitively normal by a neuropsychologist (Dr. Snitz) reviewing clinical testing data and blind to all neuroimaging data, with a mean MMSE value of 28.5 ± 1.3. All subjects provided informed consent for both the clinical examination and PET imaging. All studies were approved by the Human Use Subcommittee of the Radioactive Drug Research Committee and the Institutional Review Board of the University of Pittsburgh.

2.2. Imaging studies

Prior to PiB-PET, a structural 3 T spoiled-gradient-recalled-MR was obtained for each subject for co-registration and region-of-interest (ROI) definition. MRI scanning was performed using a GE Signa 1.5 T scanner (GE Healthcare, Waukesha, WI) and a standard head coil (Price et al., 2005) including fluid-attenuated inversion recovery (echo time = 172 milliseconds (ms), repetition time = 9004 ms) and spoiled echo gradient (echo time = 5 ms, repetition time = 25 ms) images.

[^{11}C]PiB was produced as previously described (Price et al., 2005). PET imaging was conducted using a Siemens/CTI ECAT HR+ (3D mode, 15.2 cm field-of-view, 63 planes, reconstructed image resolution ~6 mm FWHM). The subject's head was immobilized to minimize head motion. PiB was injected intravenously (12–15 mCi, over 20 s, specific activity ~1–2 Ci/μmol), and PET scanning was performed over 40–70 min. Analysis of the PiB-PET data resulted in regional standardized uptake value ratios (SUVRs) computed using cerebellum as reference (determined 50–70 min post-injection) (McNamee et al., 2009). SUVRs referenced to pons were also computed.

The baseline full resolution MRIs were resliced along the AC–PC line and down-sampled to PET voxel space. After addressing any motion artefact, the PiB-PET data were summed to form a static image and co-registered to the down-sampled FLAIR MR image.

2.3. Region of interest analysis

2.3.1. Region of interest analysis

Two types of ROIs were generated. First, ROIs of consistent dimensions (oval shape, 8.87 cm^3) (referred to as "standardized" ROIs) were created. These standardized ROIs were placed over areas anterior and posterior to the lateral ventricles, in areas where periventricular WMH caps are characteristically seen, using the downsampled FLAIR MRIs. These ROIs were of consistent size for all subjects, regardless of WMH burden or size (Fig. 1). A second ROI analysis was generated by tracing areas of obvious, discrete periventricular WMH (referred to as "hand-traced" ROIs). In this hand-traced analysis, standardized ROIs were used in areas without clearly demarcated WMH. All ROIs were created and placed by a single investigator (AEG, Fig. 1).

2.3.2. Subject specific white matter maps

We used an automated intensity-based segmentation method, with a 3-class model (gray matter, white matter, and cerebrospinal fluid) to identify the white matter on the MPRAGE image. This white matter mask was registered to the PIB-PET space using a 12-parameter affine registration, with the normalized mutual information cost function (Jenkinson et al., 2002). The T2-weighted FLAIR image was used to segment this white matter mask into WMH, and normal appearing white matter (NAWM). The automated WMH segmentation method (Wu et al., 2006) is an iterative algorithm that involves an automated selection of "seeds" of possible WMH lesions and fuzzy connectedness, which clusters voxels based on their adjacency and affinity, to segment WMH lesions around the seeds (Udupa et al., 1997). These subject-specific maps WMH maps were then co-registered to the MPRAGE images, and to PiB-PET space (using the transformation from MPRAGE to PiB-PET space), and mean SUVR values were calculated for the WMH ROIs, and for the remaining white matter (NAWM).

2.4. Classification of WMH

Participants were stratified into two groups, high WMH and low WMH, based on the visual classification of WMH based on the Cardiovascular Health Study (CHS) visual ratings of WMH (Longstreth et al., 1996). White matter changes were visually estimated and compared to standards by the total extent of periventricular and subcortical white-matter signal abnormality on axial FLAIR images and graded by successive increase from barely detectable (Grade 1) to almost all white matter involved (Grade 9) (Yue et al., 1997), these ratings were performed by two experienced clinicians (WEK and OLL). A WMH grade ≥3 was considered to have high WMH burden.

2.5. Statistical analyses

All statistical analyses were conducted in the Statistical Analysis System (SAS), Version 9.3. Two-sample, two-tailed t-tests were performed for between group comparisons, and tests for correlation were performed using Pearson correlations.

3. Results

3.1. Region of interest analysis

Significantly lower PiB retention was observed in periventricular areas in subjects with visual rating scores indicating high WMH ($p < 0.05$). In both anterior and posterior ROIs there was significantly lower PiB retention when those with high WMH were compared to those with low WMH (Figs. 1 and 2), which was seen using both the hand-traced (Fig. 2A) and standardized ROI analyses (Fig. 2B). There were no consistent differences observed between PiB uptake the anterior and posterior periventricular regions in any of the ROI analyses. Further, there was a significant relationship between PiB SUVR in the WM ROIs and the visual WM rating scores, with higher scores (more WMH) being correlated with lower PiB SUVR (data from standardized ROIs shown in Fig. 3). Additionally, similar results were seen when using a pons reference region (data not shown).

3.2. Subject specific white matter maps

In subjects with substantial WMH (i.e., visual grade ≥3), significantly lower PiB retention was observed in the WMH map when compared to the NAWM map (Fig. 4). This relationship could not be tested in the subjects with visual grade <3 since there was an insufficient number of WMH voxels to make the comparison statistically robust.

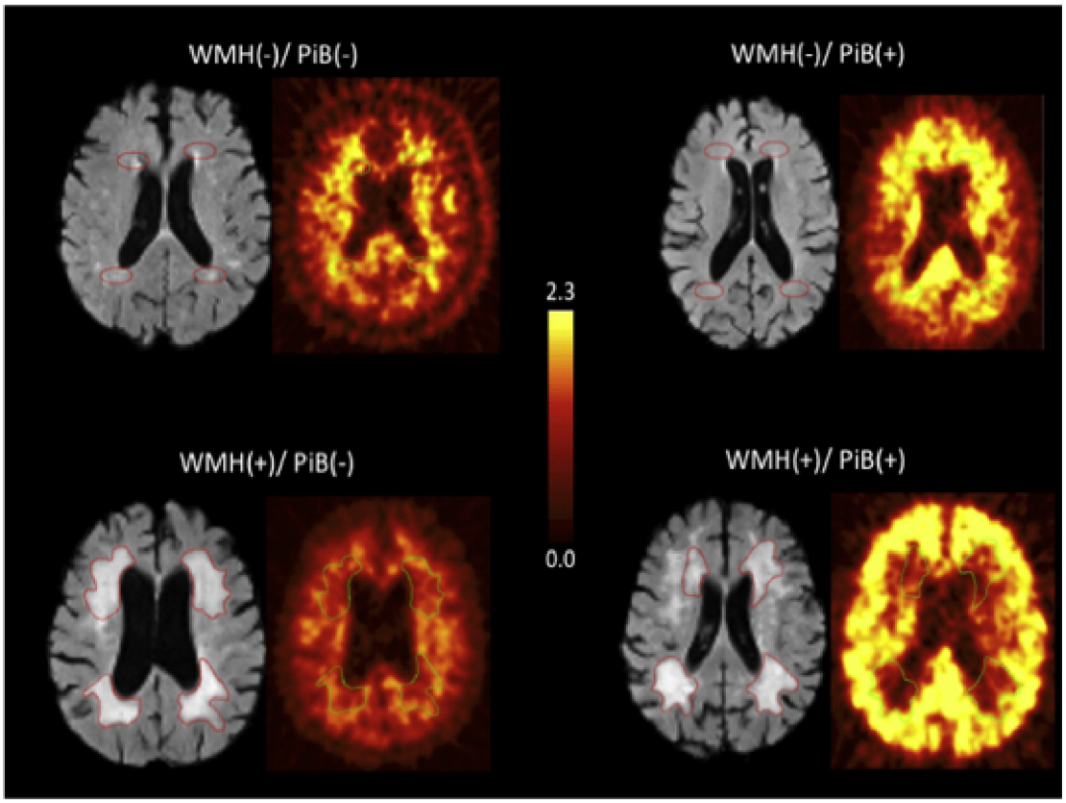

Fig. 1. Representative FLAIR MRI and PiB-PET images for WMH(−)/ PiB(−), WMH(−)/ PiB(+),WMH(+)/ PiB(−), and WMH(+)/ PiB(+). The standardized ROIs can be seen in the WMH(−) FLAIR images. The hand-traced ROIs can be seen in the WMH(+) images.

4. Discussion

In the present study PiB retention was significantly reduced in the periventricular ROIs of subjects with high WMH compared to subjects with low WMH. Additionally, in subjects with high WMH, there was significantly lower PiB retention in subject-specific maps of WMH compared to NAWM.

A simple explanation for the present findings is that a reduction in blood flow as a result of vascular disease, represented by WMH, could reduce PiB retention in the WM of individuals with significant WMH. However, we believe that this in unlikely for two reasons. First, if these changes were a result of blood flow, then it is likely that a reduction in cortical PiB would have been observed in addition to the reduction in PiB observed in the WMH and this is not the case — cortical PiB

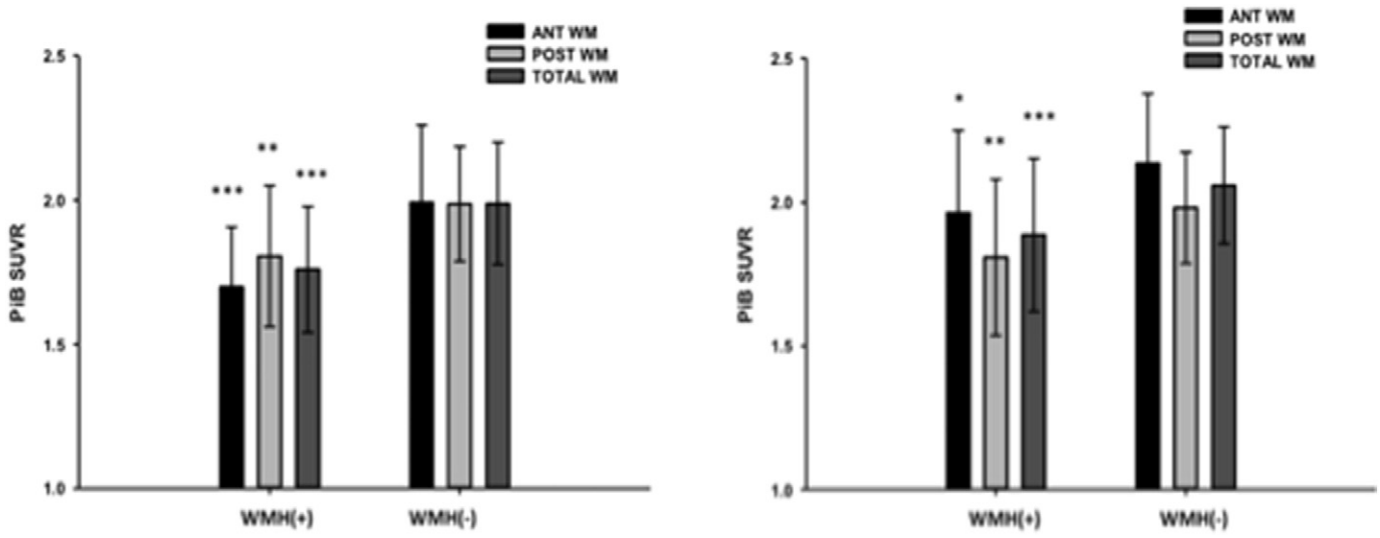

Fig. 2. (a) PiB was significantly lower in the hand-traced WMH ROIs of high WMH subjects [WMH(+)] compared to subjects with low WMH burden [WMH(−)]. (b) PiB was significantly lower in the standardized WMH ROIs of high WMH subjects [WMH(+)] compared to subjects with low WMH burden [WMH(−)]. Black bars indicate PiB retention in anterior periventricular WM, light gray bars indicate PiB retention in posterior periventricular WM, and dark gray bars indicate PiB retention in both anterior and posterior periventricular WM (total WM). ***$p < 0.001$ **$p < 0.01$ *$p < 0.05$.

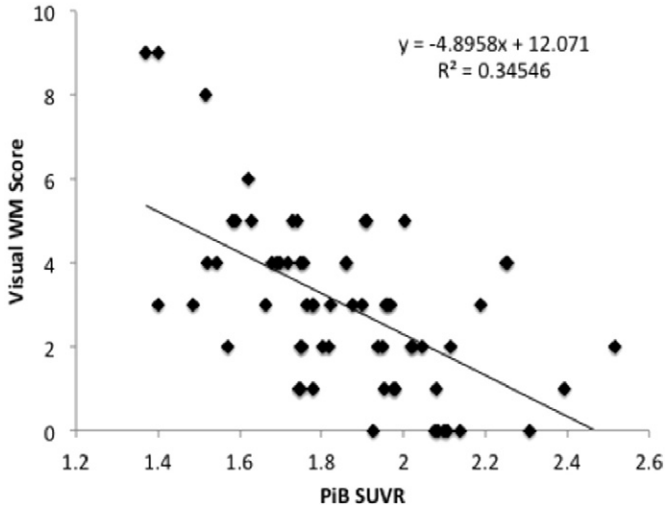

Fig. 3. PiB retention in the WMH ROIs was significantly correlated with visual WM ratings.

retention levels in both those with high and low WMH are not significantly different (data not shown). Second, when we examined regional cerebral blood flow (rCBF) using arterial spin labelling, there was no significant difference in rCBF in any of the WM ROIs between those with high and low WMH, and there was no correlation between rCBF in the WM ROIs and visual WMH rating or PiB in the WM (data not shown). Additionally, a comparison of a global cortical rCBF ROI between those with high and low WMH, showed no significant difference between the two groups.

A more likely explanation for these results is that WM in areas of WMH may have different binding characteristics to PiB than does normal WM. Indeed, Stankoff et al. (2011) have demonstrated that PiB binding in both animal and human brain sections depends on the amount of myelin present and that PiB-PET in multiple sclerosis patients showed decreased PiB binding to demyelinated lesions. The authors suggest that PiB binding to WM is at least in part related to binding to the beta-sheet structure of myelin basic protein. The data in the present study would also support this notion, as several post-mortem studies have demonstrated a degradation of myelin basic protein in areas of WMH (Murray et al., 2012; Yamamoto et al., 2009). While the molecular basis of binding of PiB to WM and WMH remains unknown, these data suggest that further exploration of this phenomenon may lead to insights about the molecular basis of this non-specific interaction.

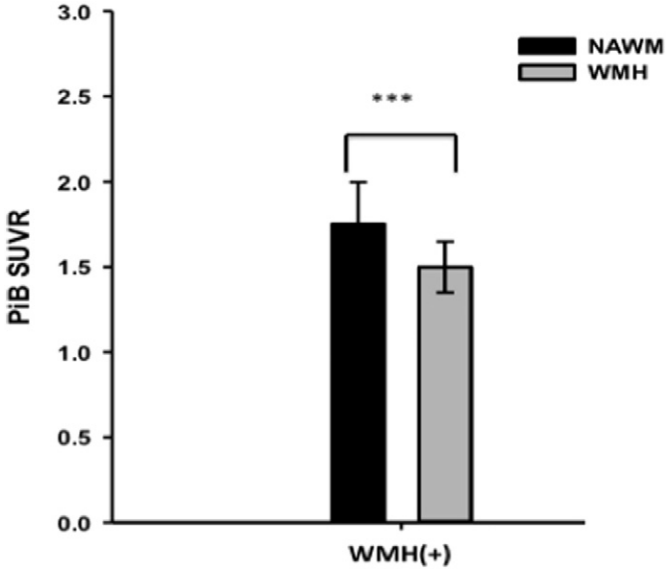

Fig. 4. PiB retention was significantly lower in the WMH maps compared to the NAWM maps in WMH(+) subjects. Black bars indicate NAWM and gray bars indicate WMH. ***$p < 0.001$.

Clinically, these results are of interest in several ways. First, as PiB has been shown to have decreased binding in areas of demyelination (Stankoff et al., 2011), these results suggest that PiB may be binding to myelin and that decreased binding in areas of WMH adds to the previous evidence of myelin damage in WMH (Murray et al., 2012; Yamamoto et al., 2009). Additionally, this study is one of few that uses amyloid tracers to study white matter. The potential for these agents to be used to study white matter is a subject that should be further explored and is of potential future clinical use. Finally, the distinction between specific cortical gray matter and non-specific white matter binding of amyloid imaging agents has been utilized clinically in visual read procedures to distinguish amyloid positive vs. amyloid negative scans. Understanding the role significant WMH play in the non-specific binding of amyloid imaging agents to WM will be of critical importance to ensure accurate visual assessment of amyloid PET scans.

From a technical perspective, the use of white matter containing reference regions for analysis of amyloid imaging data could be of concern in a population with high WMH. Further, analysis of longitudinal data utilizing WM containing regions as a reference could be challenging due to changes in WMH over time. However, because this study explored periventricular WMH and not subcortical or cerebellar white matter disease, this questions warrants further investigation. Additionally, it is possible that in participants with extensive periventricular WMH, quantification of cortical PiB may become diluted due to volume averaging, a situation that might be exacerbating by the presence of significant atrophy that might also dilute the PiB signal.

There are several limitations to this study. First, the advanced age of our cohort (>85 years) makes it difficult to make conclusions regarding PiB binding to WM in younger elderly or young adults. Additionally, it is well established that this cohort has a higher proportion of PiB-positivity (>50%) than younger, elderly cohorts (Mathis et al., 2013). This increased proportion of PiB-positives makes analysis of the effects of amyloid positivity on PiB-retention in the WM difficult because of the small number of PiB-negatives in each group. Second, the lack of partial volume correction of these data could conceivably result in reduced PiB retention particularly in periventricular areas in subjects with WMH.

This study is among the first to demonstrate that PiB appears to have different binding characteristics for WMH and NAWM. Recently, one study demonstrated a reduction in both glucose metabolism and PiB retention in gray matter regions connected to abnormal WM, however, PiB retention within areas with WMH was not explored (Glodzik et al., 2014). While further molecular study regarding the molecular basis of this interaction is needed, it is possible that PiB binding to myelin basic protein underlies the Aβ-independent interaction of PiB to WM, and because WMH contain degraded myelin basic protein, this may result in a disruption of the interaction between PiB and WM.

Conflicts of interest

GE Healthcare holds a license agreement with the University of Pittsburgh. Drs. Klunk and Mathis are co-inventors of PiB and, as such, have a financial interest in this license agreement. GE Healthcare provided no grant support for this study and had no role in the design or interpretation of results or preparation of this manuscript. All other authors have no conflicts of interest with this work.

Acknowledgments

This work was supported by NIH: K01 AG037562 (ADC); P01 AG025204 (WEK); R37 AG025516 (WEK); P50 AG005133 (OLL); and T32 MH16804 (AEG).

References

Chimowitz, M.I., Estes, M.L., Furlan, A.J., Awad, I.A., 1992. Further observations on the pathology of subcortical lesions identified on magnetic resonance imaging. Arch. Neurol. 49 (7), 747–752. http://dx.doi.org/10.1001/archneur.1992.00530310095018149750 3.

Cohen, A.D., Rabinovici, G.D., Mathis, C.A., Jagust, W.J., Klunk, W.E., Ikonomovic, M.D., 2012. Using Pittsburgh Compound B for in vivo PET imaging of fibrillar amyloid-beta. Adv. Pharmacologist 64, 27–81.

de Leeuw, F.E., de Groot, J.C., Achten, E., Oudkerk, M., Ramos, L.M., Heijboer, R., Hofman, A., Jolles, J., van Gijn, J., Breteler, M.M., 2001. Prevalence of cerebral white matter lesions in elderly people: a population based magnetic resonance imaging study. The Rotterdam Scan Study. J. Neurol. Neurosurg. Psychiatry 70 (1), 9–14. http://dx.doi.org/10.1136/jnnp.70.1.911118240.

DeKosky, S.T., Fitzpatrick, A., Ives, D.G., Saxton, J., Williamson, J., Lopez, O.L., Burke, G., Fried, L., Kuller, L.H., Robbins, J., et al., 2006. The ginkgo evaluation of memory (GEM) study: design and baseline data of a randomized trial of Ginkgo biloba extract in prevention of dementia. Contemp. Clin. Trials 27 (3), 238–253. http://dx.doi.org/10.1016/j.cct.2006.02.00716627007.

Glodzik, L., Kuceyeski, A., Rusinek, H., Tsui, W., Mosconi, L., Li, Y., Osorio, R.S., Williams, S., Randall, C., Spector, N., et al., 2014. Reduced glucose uptake and Abeta in brain regions with hyperintensities in connected white matter. Neuroimage 100, 684–691. http://dx.doi.org/10.1016/j.neuroimage.2014.06.06024999038.

Gorelick, P.B., Scuteri, A., Black, S.E., Decarli, C., Greenberg, S.M., Iadecola, C., Launer, L.J., Laurent, S., Lopez, O.L., Nyenhuis, D., et al., 2011. Vascular contributions to cognitive impairment and dementia: a statement for healthcare professionals from the American Heart Association/American Stroke Association. Stroke; J. Cereb. Circ. 42 (9), 2672–2713. http://dx.doi.org/10.1161/STR.0b013e318229496217784 38.

Jenkinson, M., Bannister, P., Brady, M., Smith, S., 2002. Improved optimization for the robust and accurate linear registration and motion correction of brain images. Neuroimage 17 (2), 825–841. http://dx.doi.org/10.1006/nimg.2002.113212377157.

Klunk, W.E., Price, J.C., Lopresti, B.J., Debnath, M.L., Holt, D.P., Wang, Y.M., Huang, G.F., Shao, L., Meltzer, C., DeKosky, S.T., et al., 2004. Human amyloid-imaging studies in controls, mild cognitive impairment and Alzheimer's disease using Pittsburgh compound-B. Neurobiol. Aging 25, S58.

Longstreth Jr., W.T., Manolio, T.A., Arnold, A., Burke, G.L., Bryan, N., Jungreis, C.A., Enright, P.L., O'Leary, D., Fried, L., 1996. Clinical correlates of white matter findings on cranial magnetic resonance imaging of 3301 elderly people. The Cardiovascular Health Study. Stroke; J. Cereb. Circ. 27 (8), 1274–1282. http://dx.doi.org/10.1161/01.STR.27.8.12748711786.

Mathis, C.A., Kuller, L.H., Klunk, W.E., Snitz, B.E., Price, J.C., Weissfeld, L.A., Rosario, B.L., Lopresti, B.J., Saxton, J.A., Aizenstein, H.J., et al., 2013. In vivo assessment of amyloid-beta deposition in nondemented very elderly subjects. Ann. Neurol. 73 (6), 751–761. http://dx.doi.org/10.1002/ana.2379723596051.

McNamee, R.L., Yee, S.H., Price, J.C., Klunk, W.E., Rosario, B., Weissfeld, L., Ziolko, S., Berginc, M., Lopresti, B., Dekosky, S., et al., 2009. Consideration of optimal time window for Pittsburgh compound B PET summed uptake measurements. J. Nucl. Med. 50 (3), 348–355. http://dx.doi.org/10.2967/jnumed.108.05761219223409.

Munoz, D.G., Hastak, S.M., Harper, B., Lee, D., Hachinski, V.C., 1993. Pathologic correlates of increased signals of the centrum ovale on magnetic resonance imaging. Arch. Neurol. 50 (5), 492–497. http://dx.doi.org/10.1001/archneur.1993.00540050044013848940 5.

Murray, M.E., Vemuri, P., Preboske, G.M., Murphy, M.C., Schweitzer, K.J., Parisi, J.E., Jack Jr., C.R., Dickson, D.W., 2012. A quantitative postmortem MRI design sensitive to white matter hyperintensity differences and their relationship with underlying pathology. J. Neuropathol. Exp. Neurol. 71 (12), 1113–1122. http://dx.doi.org/10.1097/NEN.0b013e318277387e23147507.

Price, J.C., Klunk, W.E., Lopresti, B.J., Lu, X., Hoge, J.A., Ziolko, S.K., Holt, D.P., Meltzer, C.C., Dekosky, S.T., Mathis, C.A., 2005. Kinetic modeling of amyloid binding in humans using PET imaging and Pittsburgh Compound-B. J. Cereb. Blood Flow Metab. 25 (11), 1528–1547. http://dx.doi.org/10.1038/sj.jcbfm.960014615944649.

Scarpelli, M., Salvolini, U., Diamanti, L., Montironi, R., Chiaromoni, L., Maricotti, M., 1994. MRI and pathological examination of post-mortem brains: the problem of white matter high signal areas. Neuroradiology 36 (5), 393–398. http://dx.doi.org/10.1007/BF006121267936183.

Scheltens, P., Barkhof, F., Leys, D., Wolters, E.C., Ravid, R., Kamphorst, W., 1995. Histopathologic correlates of white matter changes on MRI in Alzheimer's disease and normal aging. Neurol. 45 (5), 883–888. http://dx.doi.org/10.1212/WNL.45.5.8837746401.

Stankoff, B., Freeman, L., Aigrot, M.S., Chardain, A., Dollé, F., Williams, A., Galanaud, D., Armand, L., Lehericy, S., Lubetzki, C., et al., 2011. Imaging central nervous system myelin by positron emission tomography in multiple sclerosis using [methyl-(1) (1)C]-2-(4′-methylaminophenyl)- 6-hydroxybenzothiazole. Ann. Neurol. 69 (4), 673–680. http://dx.doi.org/10.1002/ana.2232021337603.

Thanprasertsuk, S., Martinez-Ramirez, S., Pontes-Neto, O.M., Ni, J., Ayres, A., Reed, A., Swords, K., Gurol, M.E., Greenberg, S.M., Viswanathan, A., 2014. Posterior white matter disease distribution as a predictor of amyloid angiopathy. Neurology 83 (9), 794–800. http://dx.doi.org/10.1212/WNL.0000000000000732250637 59.

Udupa, J.K., Wei, L., Samarasekera, S., Miki, Y., van Buchem, M.A., Grossman, R.I., 1997. Multiple sclerosis lesion quantification using fuzzy-connectedness principles. I.E.E.E. Trans. Med. Imaging 16 (5), 598–609. http://dx.doi.org/10.1109/42.6407509368115.

Wu, M., Rosano, C., Butters, M., Whyte, E., Nable, M., Crooks, R., Meltzer, C.C., Reynolds 3rd, C.F., Aizenstein, H.J., 2006. A fully automated method for quantifying and localizing white matter hyperintensities on MR images. Psychiatry Res. 148 (2–3), 133–142. http://dx.doi.org/10.1016/j.pscychresns.2006.09.00317097277.

Yamamoto, Y., Ihara, M., Tham, C., Low, R.W., Slade, J.Y., Moss, T., Oakley, A.E., Polvikoski, T., Kalaria, R.N., 2009. Neuropathological correlates of temporal pole white matter hyperintensities in CADASIL. Stroke; J. Cereb. Circ. 40 (6), 2004–2011. http://dx.doi.org/10.1161/STROKEAHA.108.52829919359623.

Yoshita, M., Fletcher, E., Harvey, D., Ortega, M., Martinez, O., Mungas, D.M., Reed, B.R., DeCarli, C.S., 2006. Extent and distribution of white matter hyperintensities in normal aging, MCI, And AD. Neurology 67 (12), 2192–2198. http://dx.doi.org/10.1212/01.wnl.0000249119.95747.1f17190943.

Young, V.G., Halliday, G.M., Kril, J.J., 2008. Neuropathologic correlates of white matter hyperintensities. Neurology 71 (11), 804–811. http://dx.doi.org/10.1212/01.wnl.0000319691.50117.5418685136.

Yue, N.C., Arnold, A.M., Longstreth Jr., W.T., Elster, A.D., Jungreis, C.A., O'Leary, D.H., Poirier, V.C., Bryan, R.N., 1997. Sulcal, ventricular, and white matter changes at MR imaging in the aging brain: data from the cardiovascular health study. Radiology 202 (1), 33–39. http://dx.doi.org/10.1148/radiology.202.1.89881898988189.